Environmental Engineering and Management Journal

December 2021, Vol. 20, No. 12, 1893-1903
http://www.eemj.icpm.tuiasi.ro/; http://www.eemj.eu

"Gheorghe Asachi" Technical University of Iasi, Romania

AMINO-FUNCTIONALIZED MESOPOROUS MATERIALS USED FOR CO_2 ADSORPTION

Silvana Borcănescu[1*], Alexandru Popa[1], Danica Bajuk-Bogdanović[2], Ivanka Holclajtner-Antunović[2], Snežana Uskoković-Marković[3]

[1]"Coriolan Drăgulescu" Institute of Chemistry, 24 Mihai Viteazul Blvd., 300223 Timișoara, Romania
[2]Faculty of Physical Chemistry, University of Belgrade, P.O. Box 47, 11158 Belgrade, Serbia
[3]Faculty of Pharmacy, University of Belgrade, P.O. Box 146, 11221 Belgrade, Serbia

Abstract

In this paper CO_2 adsorption over SBA-15 and MCM-41 molecular sieves functionalized by grafting technique with 3-aminopropyl-triethoxy silane was investigated. Starting from commonly used SBA-15 molecular sieve a different sample named SSBA-15 was synthesized by tetraethyl orthosilicate hydrolysis using P123 block copolymer as surfactant and 1-phenyldecane as expansion agent. The surface of SSBA-15 molecular sieve was modified by two ways synthesis steps: first using (3-Glycidyloxypropyl) trimethoxysilane and second by introduction of ethylene diamine (N2) as an amination agent. The prepared amino-functionalized mesoporous materials were further characterized by different investigation methods: FT-IR spectrometry, X-ray diffraction analysis, SEM-EDX, nitrogen physisorption analysis at 77 K. Adsorption-desorption measurements towards CO_2 were investigated using Temperature-Programmed desorption (TPD). In order to find the optimum value of the adsorption–desorption process, the influence of temperature in the range of 50-80°C was followed. Using a combination of mass spectrometry and thermogravimetry the resulted gases during the adsorption–desorption process of CO_2 were identified. Compared to already published literature, the herein reported results of the studied amino functionalized sieves for CO_2 adsorption-desorption process are significantly better and can be considered as promising. The best results obtained in case of MCM-41-sil were further investigated by adsorption-desorption cycles.

Key words: adsorption-desorption cycles, adsorbent efficiency, CO_2 adsorption, molecular sieves grafted, temperature influence

Received: September, 2020; Revised final: October, 2021; Accepted: October, 2021; Published in final edited form: December, 2021

1. Introduction

Considering the growth of industrialization development and increasing emission of CO_2 in the atmosphere, it is necessary to constantly work on improving the adsorptive properties of porous materials for carbon dioxide adsorption, usually by modifying their surfaces. Mesoporous materials have been used as adsorbents, catalysts supports and heterogeneous catalysts in various applications as shown by Abolfazl et al. (2012) and Sheng et al. (2014). In the last years, the research area has been focused on the CO_2 adsorption solutions regarding this direction. It is very important to develop effective methods for this purpose. Suitable adsorbents for CO_2 should combine several properties such as: good adsorption capacity, high selectivity and high stability (Harja et al., 2021; Zang et al., 2019). From the literature data, it is found that mesoporous materials such as SBA-15 (Khader et al., 2015; Ma et. al., 2009; Sayari et al., 1998; Son et al., 2008) and MCM-41 (Heydari-Gorji et al., 2011; Son et al., 2008) with well-ordered structures were applied for different applications (Barbosa et al., 2011; Ciesla and Schuth, 1999; Doadrio et al., 2004; Manianglung et al., 2019) due to good performances. These materials are characterised by a uniform hexagonal cylindrical pore system, tunable pore size (15-100 Å), high surface

* Author to whom all correspondence should be addressed: e-mail: silvana.borcanescu@gmail.com

area (>700 m^2/g), large pore volume (≥0.7 cm^3/g), large number of silanol groups (~40–60%), negligible pore blocking effect, high surface reactivity, and good hydrothermal, chemical and mechanical stability (Beck et al., 1992; Selvam et al., 2001). Investigations by Zhao et al. (1998), have shown that SBA-15 also possess some of the desirable properties, such as large surface area (600–1000 m^2/g), well-defined pore structure with variable pore diameters (50-300 Å) and a highly ordered hexagonal mesostructured.

By functionalizing the surface of these materials with different organic groups (thiol, vinyl, amine, phenyl, propyl) has attracted much attention in recent years as reported by Wang et al. (2004), Wang et al. (2006) and Popa et al. (2018). Thus, amine functionalized mesoporous silica presents a very good capture for CO_2 due to a very high selectivity towards CO_2 at a low partial pressure, a wide range of temperature as demonstrated by Gargiulo et al. (2014), Sánchez-Zambrano et al. (2018) and Sharma et al. (2012), and, an controlled pore size, and easy surface modification using functionalization agents (Asefa and Tao, 2012; Chen et al., 2017; Zelenak et al., 2008).

These materials have recently emerged as a promising class of solid adsorbents that can effectively adsorb CO_2, and may be used in a variety of approaches as demonstrated Bollini et al. (2011) and Galarneau et al. (2003). Na Rao et al. (2018) obtained maximum CO_2 adsorption capacities of 3.53 $mmol/g^{-1}$ for 50%-PEI-MCM-41 and 2.41 $mmol/g^{-1}$ (50%-APTS-MCM-41) at 25 °C and 1 atm. The samples graphed with aminopropyl (AP), ethylenediamino (ED) and diethylenetriamino (DT) showed amine efficiencies in CO_2 capture up to 0.38 mol CO_2/ mol N leading to uptakes of CO_2 ranging between 38.2-76.9 mg CO_2/mol N obtained at 45°C and 1 bar pressure (Sanz et al., 2015). Carvalho et al. (2015) studied the impregnation of SMCM-41 adsorbent material obtained from sand compared to MCM-41, using mono and diethanolamine amines (MEA and DEA) at different concentrations for CO_2 adsorption performance. The best CO_2 adsorption capacity was achieved for MCM-41 (1.39 mmol g^{-1}) and SMCM-41 (10.40 mmol g^{-1}) for 3% MEA impregnation at 1 bar pressure. In the case of 3% MEA and pressures closed to 1 bar it proved that the adsorption results are much more satisfactory compare to pure MCM-41 and SMCM-41.

The present study was carried out to find out how the temperature influences the CO_2 adsorption-desorption process on amino functionalized SBA-15 and MCM-41. The gases resulting during the adsorption–desorption process of CO_2 on the prepared materials were identified using mass spectrometry combined with thermal analysis technique. The best results obtained are going to be further investigated by adsorption-desorption cycles in order to establish the regeneration capacity of the molecular sieves.

2. Experimental

2.1. Preparation of molecular sieves

MCM-41 molecular sieve was prepared by the method presented in the literature data by Beck et al. (1992), while SBA-15 was synthesized following the procedure published by Zhao et al. (1998). These molecular sieves were functionalized by grafting, using 3-aminopropyl-triethoxy silane (APTES) as a functionalization agent. The preparation method of the functionalized materials for obtaining 1 g of molecular sieves is previously described by Borcanescu et al. (2019). The prepared compounds were denoted as: MCM-41-sil and SBA-15-sil.

A modified SBA-15 sample named SSBA-15 was prepared by the following procedure: tetraethyl orthosilicate (TEOS) was first hydrolysed by P123 block copolymer used as surfactant and 1-phenyldecane as expansion agent. The reaction steps for synthesis of SSBA-15 were reported in previous paper (Borcanescu et al., 2019). The difference between the synthesis of SSBA-15 and of SBA-15 is the presence of 1-phenyl-decane used as expansion agent. First step in the synthesis of modified SSBA-15 was to use a silane coupling agent, (3-Glycidyloxypropyl)trimethoxysilane, and secondary an amination reagent: ethylene diamine (N2). This compound was denoted as SSBA-15+N2. In all the cases, the role of the amine was to improve the CO_2 adsorption capability.

2.2. Characterization methods

Infrared spectra of the mesoporouse materials were recorded on a Jasco FTIR 430 spectrometer. The prepared materials were recorded in the 4000–400 cm^{-1} range, using the KBr pellets. The phase compositions of the projected molecular sieves were performed on a Bruker D8 Advance powder diffractometer. This measurement instrument was equipped with a copper target X-ray tube in the range $2\theta=0.5\div5$. Textural characteristics of the outgassed samples were collected using a Quantachrome Nova 2000 series with N2 isotherms obtained at 77 K. Specific surface was calculated based on BET (Brunauer–Emmet–Teller) method. The cumulative pore volume was calculated by the BJH (Barrett-Joyner-Halenda) method and adsorption pore volume V_PN_2 was determined based on the adsorption isotherm obtained results. The morphology of the molecular sieves and amino-functionalized mesoporous materials was investigated using high-performance scanning electron microscope JEOL JSM-6610LV low vacuum SEM at the following conditions: 15 kV acceleration voltage, 20 nA beam current and 1 mm spot size. The samples were coated by ion sputtered gold layers using Leica EM SCD005 sputter coater.

The behaviour during heating process of the

obtained functionalized materials has been monitored by thermal analysis using TGA/SDTA 851-LF 1100 Mettler Toledo. This apparatus system was coupled with a Pfeiffer Vacuum Thermo Star GSD320 mass spectrometer equipped with a 200 °C silica capillary. The description of the adsorption-desorption measurements was presented in detail by Borcănescu et al. (2019).

Each sample was pre-treated in flowing N_2 at 150°C. The investigated mesoporouse molecular sieves were cooled to the desired adsorption temperature range 50 - 80°C, and exposed to 30% mixture of gases CO_2/N_2 (70 mL min^{-1}) for 90 min. The desorption step took place in the range of 60-180°C. Temperature rate was increased with 10°C min^{-1} and the isothermal treatment was performed at 180°C for 30 min. The best promising results obtained for the tested adsorbents were further investigated by adsorption-desorption cycles in order to study the stability and renderability of the compounds.

The sample tested for the adsorption – desorption cycles was pre-treated in flowing N_2 at 120°C. The investigated molecular sieves were then cooled to the desired adsorption temperature (60°C), and further exposed to 30% CO_2/N_2 (70 mL min^{-1}) mixture of gases for 30 min. These steps were repeated several times with an increase of the temperature rate with 10°C min^{-1}.

3. Results and discussion

3.1. Infrared spectroscopy

The FT-IR spectra of the studied functionalized materials were recorded in order to identify the functional groups anchored on the surface of the prepared molecular sieves. For all the spectra (Fig.1), four characteristic bands were identified between 1090 and 460 cm^{-1}. These intensities can be associated with Si–O–Si stretching vibrations corresponding to silica condensed networks. The broad absorption band around 3440 cm^{-1}, in all the spectra, can be associated with OH stretching due to the water molecules adsorbed onto hydrogen bonded silanol groups, indicating that the silica framework is hydrophilic.

The FT-IR spectrum of the parent MCM-41 is evidenced by the following peaks: 1230 cm^{-1} (shoulder) and 1081 cm^{-1} which are characteristic peaks of stretching vibration of the Si–O–Si bond; a characteristic peak is observed at 795- 800 cm^{-1} corresponding to Si-O-Si stretching vibrations; and a peak is found at 461 cm^{-1} corresponding to banding vibration. After modification with APTES, the MCM-41 still retained its siliceous structure, but some additional bands are observed at 697 cm^{-1}. The weak peak can be attributed to the bending of N-H bonds. The bending vibrations present at 1589 cm^{-1} corresponds to symmetrical $-NH_3^+$. The presence of these two bands confirms the existence of amine groups (Kamarudin et al., 2013). Further, the small band present around 1484 cm^{-1} attributed to $–NH_3^+$ stretching vibration in the case of MCM-41-sil and SBA-15-sil composites, confirms the grafting of APTES, used as a functionalization agent on silica composites (Fig. 1) (Maria Chong and Zhou, 2003).

The spectrum of SSBA-15+N2 is characterized by typical bands of stretching vibrations of Si-O-Si groups in the silica structure, which appear at 1080, 800 and 461 cm^{-1}. The broad absorption band centred at 3369 - 3418 cm^{-1}, and a weak absorption band at 1636 cm^{-1}, indicate the presence of water due to the absorbed water molecules in the sample, and belong to the bending vibrations of H-O-H. In case of SSBA-15+N2 the FT-IR band present at 1522 cm^{-1} can be assigned to N–H stretching, the band present at 795 cm^{-1} can be attributed to N–H bending vibrations respectively. Thus the stretching frequencies evidence the successful grafting procedure of ethylene diamine on SSBA-15 molecular sieve.

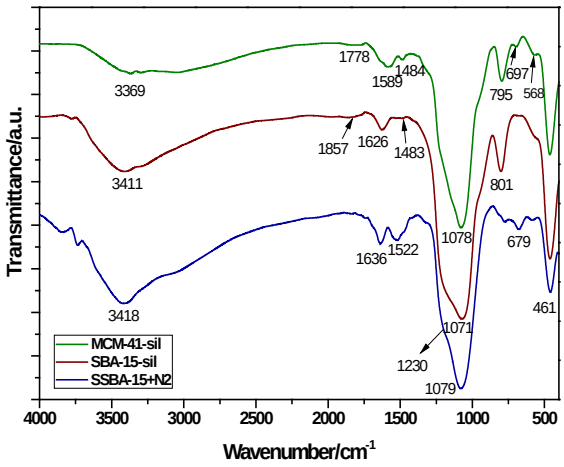

Fig. 1. FTIR spectra of MCM-41-sil, SBA-15-sil and SSBA-15+N2 functionalized materials

3.2. X-ray diffraction spectra analysis

According to the X-ray diffraction analysis results, SBA-15 and SSBA-15 samples presents hexagonal structure, being evidenced by the three diffraction peaks present at the following low angles: 0.98°, 1.62° and 1.83°. These diffraction peaks corresponds to (100), (110) and (200) Miller crystal planes. In the functionalized sample denoted SBA-15-sil, the diffraction peaks are shifted to lower angles compared to SBA-15 sample without functionalization (Fig. 2). This is due to the widening of the silica frameworks (increases the lattice parameter) during functionalization. The X-ray diffraction spectra of both composites indicate well-ordered hexagonal pore arrangement and characteristics of SBA-15 type material. XRD patterns of the aminated SSBA-15 sample exhibited three clear peaks characteristic of hexagonally ordered structure, but relative intensities of (110) and (200) peaks to the (100) peak are decreasing compared to parent SSBA-15. This may indicate that order of the mesopores decreases when the sample is modified.

Recently published study has shown that the hexagonal structure of MCM-41 mesoporous material

is also confirmed by the presence of the characteristic diffraction peaks at low angles. The MCM-41 structure is preserved and after the functionalization process. After introduction of amine groups through the amination agent, the diffraction peaks characteristic for MCM-41 mesoporous material were only marginally shifted to higher values. This information is in accordance with the decrease of pore size and surface area of the composite (Meléndez-Ortiz et al., 2014).

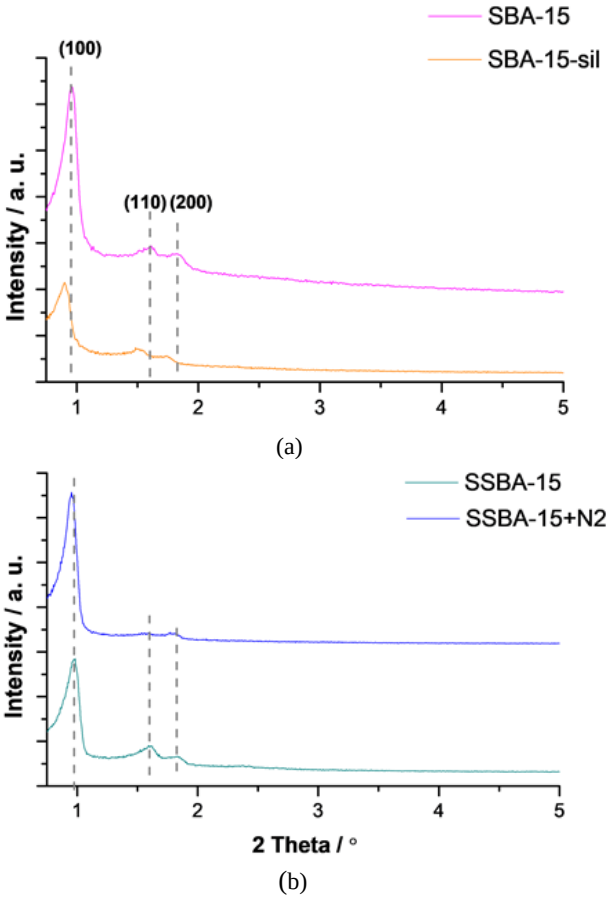

Fig. 2. X-ray diffraction spectra of SBA-15, SBA-15-sil, SSBA-15 (a) and SSBA-15+N2 (b) functionalized materials

3.3. Specific surface area

The isotherms of studied functionalized samples could be classified as type IV isotherms with H1 hysteresis loops, a typical characteristic of mesoporous materials, according to some of the isotherms reported in the previous research (Kamarudin et al., 2013; Sánchez-Zambrano et al., 2018) and to the IUPAC classification (Rodrıguez-Estupinan et al., 2015). The main textural parameters like specific surface area, pore volume and an average pore diameter were calculated from the N_2 adsorption isotherm.

The experimental data of textural parameters are presented in Table 1. In case of SBA-15-sil molecular sieve, surface area and pore volume are decreased approximately to half of the SBA-15 textural characteristics: specific surface area from 725.0 to 288.8 m^2/g and pore volume from 1.99 to 0.664 cm^3/g as can be seen from Table 1. This decrease process of the textural parameters can be due to the functionalization process. More probably the APTES ligand reacts with the silanol groups located at the both external and internal surface openings of the pores, resulting in the restriction of the diffusion of nitrogen molecules as Majda et al. (2016) demonstrated. The data also reveal that the surface area and the pore volume of MCM-41 decrease after modification with 3-aminopropyl-triethoxy silane to 655.8 m^2/g and to 0.611 cm^3/g, respectively, due to the increasing number of silica particles and/or occupation of the pores. However, the highest decrease of surface area and pore volume is achieved for SSBA-15+N2.

3.4. SEM analysis

The morphologies of the representative synthesized functionalized materials were investigated using SEM. SSBA-15 presents the rope-like structure with an average diameter below 1 μm as can be noted from SEM images presented in Fig. 3. SBA-15 presents the same rope-like structure also as Ratchadapiban et al. (2018) had demonstrated. The structure can be aggregated into a highly ordered and aligned macroscopic structure. The surface morphology in case of SSBA-15+N2 functionalized material (Fig. 3b), is practically the same, being confirmed by the results obtained from X-ray analysis mentioned above.

3.5. EDX analysis

In Table 2 are presented the results of the EDX analysis for the studied functionalized materials. Following elements such as C, O and Si are detected by EDX analysis in the molecular sieve's composition. In the case of the materials functionalized by grafting with 3-aminopropyl-triethoxy silane, weight percent of Si decreases from 47.43 % to 40.73 % (sample MCM-41 and MCM-41-sil). In case of the sample SSBA-15+N2 compared to sample SBA-15 this decrease, of Si content, is more visible due to presence of the silane bonding agent, (3Glycidyloxypropyl)trimethoxysilane, and also of the amination reagent: ethylene diamine (N2).

EDX analysis confirms the presence of N (4.59 % for MCM-41-sil, 2.90 % for SSBA-15+N2 and 2.32 % for SBA-15-sil respectively) in addition to the previous mentioned elements for the functionalized molecular sieves. After the functionalization process of the studied molecular sieves with different amination reagents, the amino functional group provided are linked on the surface of the support material. Thus, based on the obtained results we can say that the functionalization process of the mesoporouse materials took place successfully being also confirmed by the chemical results, low-angle X-ray diffraction and N_2 adsorption-desorption analysis.

Table 1. Morphology characteristics data of the studied functionalized materials

No.	*Sample*	*Specific surface area (m^2/g)*	*Pore volume BJH_{Des} (cm^3/g)*	*Average pore diameter BJH_{Des} (nm)*
1.	SBA-15	725.0	1.19	6.64
2.	SBA-15-sil	288.8	0.664	6.63
3.	SSBA-15	766.5	1.294	6.62
4.	SSBA-15+N2	224.8	0.337	5.49
5.	MCM-41	1299.7	0.695	3.30
6.	MCM-41-sil	655.8	0.611	3.25

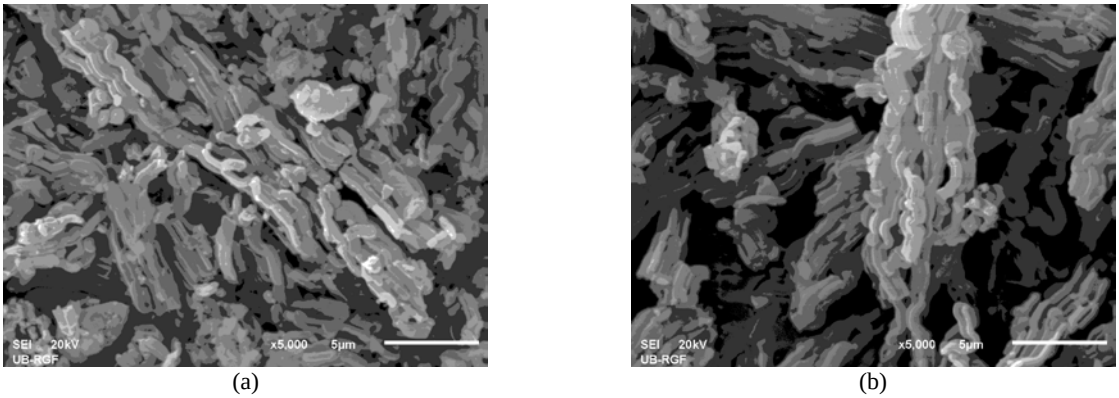

(a) (b)

Fig. 3. SEM images of a) SSBA-15 and b) SSBA-15+N2 functionalized materials

Table 2. Elemental analysis of the functionalized mesoporous materials

No.	*Sample*	*C*	*N*	*O*	*Si*
		wt%			
1.	SBA-15	-	-	50.72	49.28
2.	SBA-15-sil	36.37	2.32	44.34	16.87
3	SSBA-15	37.61	-	50.31	12.08
4.	SSBA-15+N2	36.60	2.90	48.85	11.65
5.	MCM-41	-	-	52.47	47.43
6.	MCM-41-sil	16.32	4.59	38.29	40.79

3.6. Thermal analysis

First endothermic effect present on the DTG curves below 100°C (Figs. 4-5) can be attributed to the removal of physically adsorbed water overlapped with crystallization water of the mesoporous functionalized materials. Is it is very important to notice the second endothermic effect accompanied by a major weight loss that can be observed in the temperature range of 300-500°C (Fig. 4 and Fig. 5) for all the analysed mesoporous materials. These could be assigned to small traces of P123 surfactant thermal removal process (Zhao et al., 1998) and the decomposition of 3-aminopropyl-triethoxy silane. The small endothermic effect present on DTG curve at approximately 550°C can be assigned to the dehydroxylation of the silicate networks as observed on mesoporous pure-silica materials (Kim et al., 2017) and/or the elimination of residual ethoxy groups because of incomplete hydrolysis of TEOS, as reported in literature.

In case of SSBA-15+N2 functionalized material the peaks present above 250°C can be correlated to the gradual loss of the amino propyl functional groups (Popa et al., 2018).

3.7. CO_2 adsorption and desorption investigated by TPD method

It is very important that the studied amino-functionalized materials to present promising adsorption-desorption properties and should be used in the industrial area for CO_2 removal. From this point of view the synthesized materials were investigated by the TPD method. The results of CO_2 adsorption-desorption process of functionalized materials and their isotherms at the investigated temperature (60 ^oC) and corresponding mass spectrometry analysis are presented in the figure below (Figs. 6a and 6b).

The CO_2 adsorption capacity of the adsorbent composite is express in mmol CO_2/gram of adsorbent. This mass gain can be seen from the tested sample in the adsorption process (Fig. 6a). For more accurate results the mass gain of the tested functionalized material was calculated from the thermogravimetric curves, from the mass loss during the desorption step (Fig. 6a).

The influence of CO_2 adsorption temperature over the all three functionalized materials was investigated in order to choose the optimum value for

the adsorption–desorption process. In case of the functionalized materials at 60°C termogravimetric curves of the mass gain of these samples are more representative regarding CO_2 adsorbed quantity. Ranging the TPD temperature, the CO_2 adsorbed quantity decreases as can be observed in Fig. 7.

If the temperature for CO_2 adsorption is 70 °C, the achieved results for the mass gain in the adsorption process are satisfactory for composites MCM-41-sil, SBA-15-sil and SSBA-15+N2, and the calculated values are 2.18, 1.09 and 1.73 mmol CO_2/gram SiO_2, respectively (Fig. 7). The values for CO_2 adsorption capacity of MCM-41-sil and SBA-15-sil tested at 80 °C are quite similar to the values of the composites tested at 50ºC, while in case of SSBA-15+N2 it is considerably lower (Fig. 7). The best results were obtained in case of MCM-41-sil, 3.32 mmol CO_2 and SSBA-15+N2 samples 1.96 mmol CO_2 per gram, while the optimal temperature for CO_2 adsorption–desorption by TPD results was 60 °C.

Another important parameter of the adsorption–desorption process is the adsorption efficiency of the adsorbent (expressed in mmol CO_2/mmol NH_2). The efficiency of the adsorbent was calculated with the Eq. (1):

$$Adosrption\ efficiency = \frac{adsorbed\ CO^2 (mmol\ g^{-1})}{amine\ content\ (mmol\ g^{-1})} \quad (1)$$

Through its values this parameter offers information of great interest about CO_2 adsorption of the amino incorporated groups. From the literature data it is very well known that each amination agent used for CO_2 adsorption process corresponds to an optimal synthesis temperature. This information is necessary for the adsorption process to take place. From the interaction of CO_2 with amine group's results carbamates formation, leading to the as named CO_2 zwitterion RH_2N^+–COO^-, which corresponds to 1, 3-zwitterion, where 1 and 3 represents the positive and negative centers, respectively (Ridha et al. 2020).

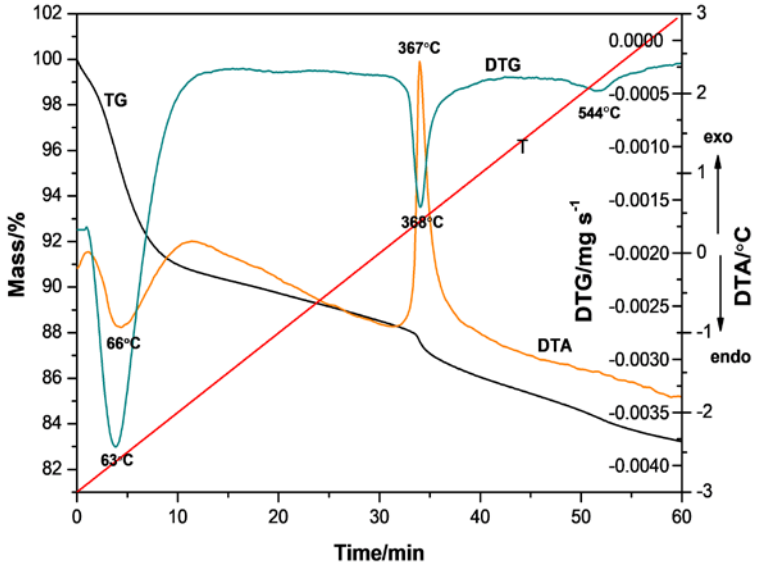

Fig. 4. TG-DTG-DTA curves of SBA-15-sil functionalized material

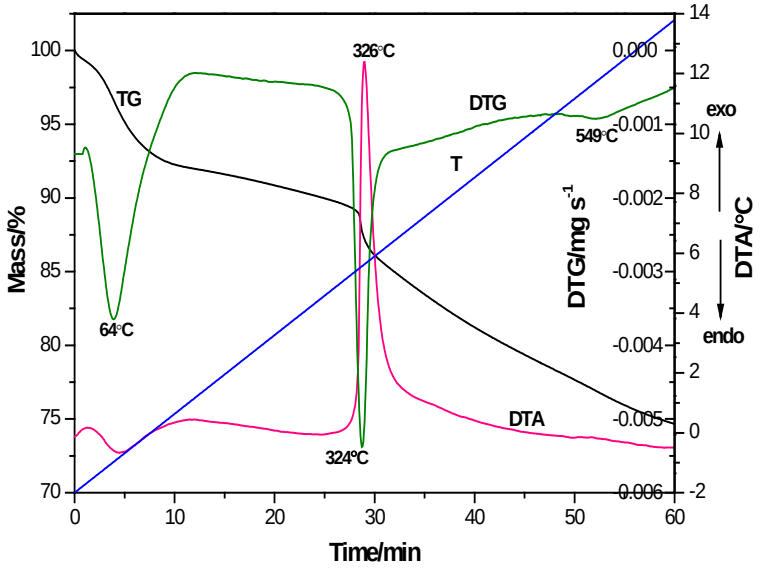

Fig. 5. TG-DTG-DTA curves of MCM-41-sil functionalized material

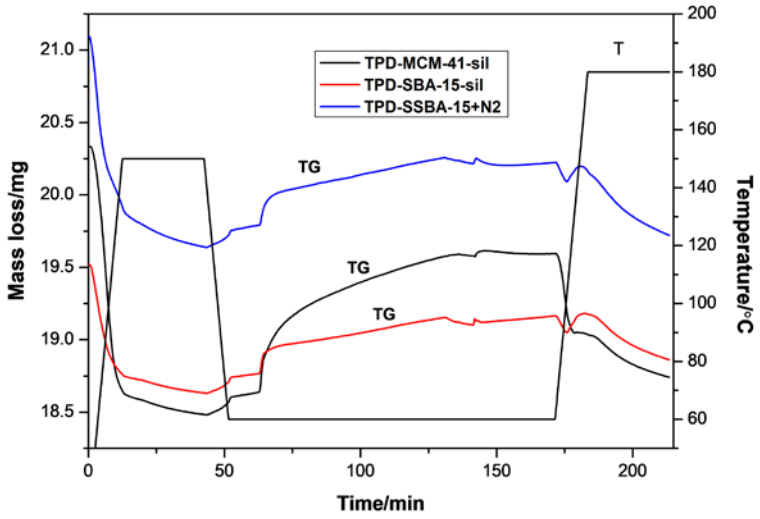

(a)

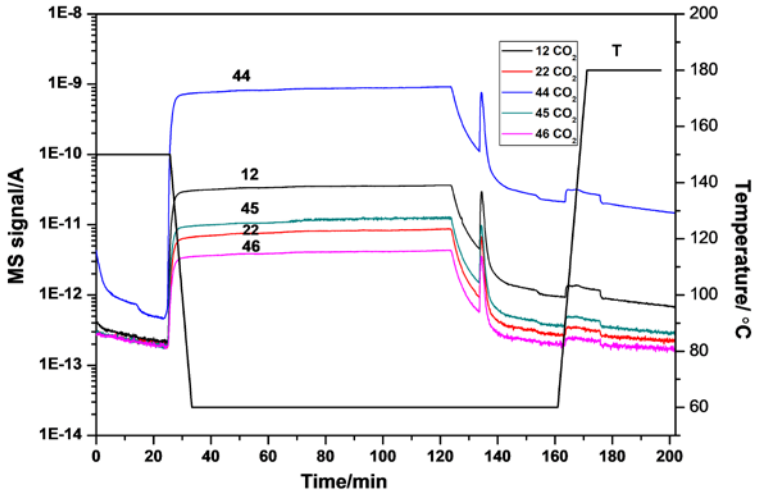

(b)

Fig. 6. TPD steps of functionalized materials MCM-41-sil, SBA-15-sil and SSBA-15+N2 and corresponding adsorption isotherms at 60 °C (a) and MS spectra for MCM-41-sil composite at 60 °C (b)

Generally, for this reaction to take place two amine groups per one CO_2 molecule is necessary. This adsorption efficiency can be defined as the CO_2/N molar ratio. The carbamate formation is a reversible chemisorption process. The best values of adsorption efficiency for all 3 studied adsorbents are obtained at 60 °C. For instance, the value of adsorption efficiency for MCM-41-sil is 0.64 mmolCO_2/mmolNH_2 and for SSBA-15+N2 is 0.55 mmolCO_2/mmolNH_2 (Fig. 7). With increasing the temperature to higher values (70-80°C) the adsorption efficiency decreases, as can be seen in Fig. 7.

The results obtained in our research group comparing to those reported in the literature (Hiyoshi et al. 2005; Yan et al. 2011) concerning the CO_2/NH_2 ratio values for the studied amino molecular sieves can be considered promising for the possible applications based on the CO_2 adsorption-desorption process.

Some of the results reported in the literature regarding mesoporous materials used for CO_2 adsorption are presented in Table 3. These support materials properties are influenced by different synthesis conditions such as: the type of amine used, the tested method and adsorption conditions.

The amine dependence efficiency with the organic loading is different for every used adsorbent. In the literature is also confirmed that the higher organic content of the double functionalized samples is in accordance with the positive effect of this method achieving higher efficiencies in CO_2 adsorption.

Ahmeda et al. (2016) studied the reactivity of monoethanolamine, diethanolamine and triethanolamine loaded on the siliceous mesoporouse materials for CO_2 adsorption at low pressure. The reactivity of these amines decreases from MEA>DEA>TEA. SBA-15 mesoporous materials with different synthesis characteristics have been synthesized by Vilarrasa-García et al. (2014). By using 3-(triethoxysilyl)propylamine as grafting agent which react with free silanol groups present on the silica surface, it was observed an improvement of CO_2 uptake to 0.64 mol CO_2/mol N. The samples have the capacity to regenerate as it can be achieved a constant activity after 3 adsorption-desorption cycles.

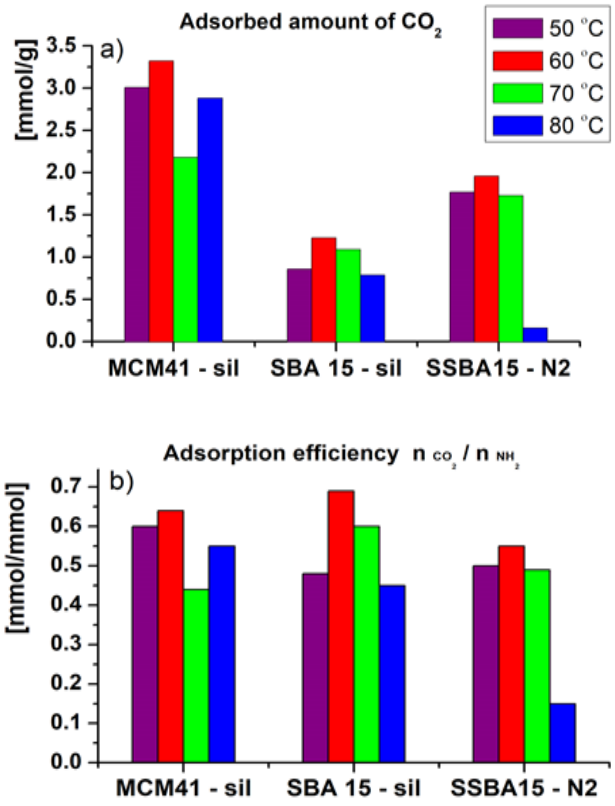

Fig. 7. The amounts of the captured CO_2 on molecular sieves a) and their adsorption efficiency b) at different temperatures

Mass spectrometry together with thermogravimetry was used to identify the resulting gases from the adsorption–desorption process of CO_2 on synthesized samples. The main compound present on the MS spectra of the graphed materials is CO_2 (Fig. 6b), and also a small amount of H_2O.

4. CO_2 adsorption-desorption cycles

A very important direction of the mesoporous materials with adsorbent properties for the industrial area is to establish the regeneration capacity of the molecular sieves. From this point of view 9 cycles of CO_2 adsorption-desorption were carried out for MCM-41-sil (Fig. 8). This sample was selected because it achieved the best value for CO_2 capture while the optimal temperature for CO_2 adsorption–desorption observed from TPD programme results was 60°C. The results show that MCM-41-sil adsorbent is fairly stable presenting a slight decrease in adsorption capacity after 9 adsorption-desorption cycles.

5. Conclusions

SBA-15 and MCM-41 mesoporous materials were successfully synthesized and grafted with 3-aminopropyl-triethoxy silane used as a functionalization agent. The X-ray diffraction spectra confirm that the functionalized materials present hexagonal structure, as can be seen from FTIR results.

Table 3. Adsorption-desorption performance of the mesoporous materials with different amine type loadings

Support	***Amine Type***	***Method***	***Adsorption conditions***	***Observation***		***Reference***
				CO_2 adsorption capacity (mg CO_2/g ads)	***adsorption efficiency (mmol CO_2/mmol N)***	
SBA-15	PEI	Impregnation	N_2 stream, 15.1v/v% CO_2 mL/min	82.2-105.2	-	Ahmeda et al. (2016)
Si-MCM-41	MEA DEA TEA	Impregnation	25° C, up to 1 bar, pure CO_2	27.78-39.3	-	Mello et al. (2011)
MCM-41	APTES	Grafting	20° C, up to 1 bar, CO_2	47	-	Mukherjee et al. (2019)
MCM-41	MEA BZA MEA	Impregnation	25-60 °C, up to 1 bar CO_2	102.98 39.96 64.69	-	Mukherjee et al. (2019)
PE-MCM-41	PEI ED DT	Grafting	45° C, 1bar	38.2-76.9	0.36-0.38	Rao et al. (2018)
PE-MCM-41	PEI TEPA PEHA	Impregnation		88.2-96.9	0.20-0.25	Rao et al. (2018)
SBA-15	APTES	Hydrotermal	25° C, up to 1 bar, pure CO_2	56.3-106.1	0.45-0.64	Vilarrasa-García et al. (2014)
SBA-15	APTMS	Grafting	25° C, up to 1 bar, CO_2	70	-	Yuan et al. (2014)
SBA-15	APTES	Grafting	25° C, up to 1 bar, CO_2	66	-	Zelenak et al. (2008)
MCM-41-sil	APTES	Grafting	60° C, 1bar	146	0.64	This work
SBA-15-sil	APTES	Grafting		54.1	0.69	This work
SSBA-15+N2	APTES	Grafting		86.2	0.55	This work

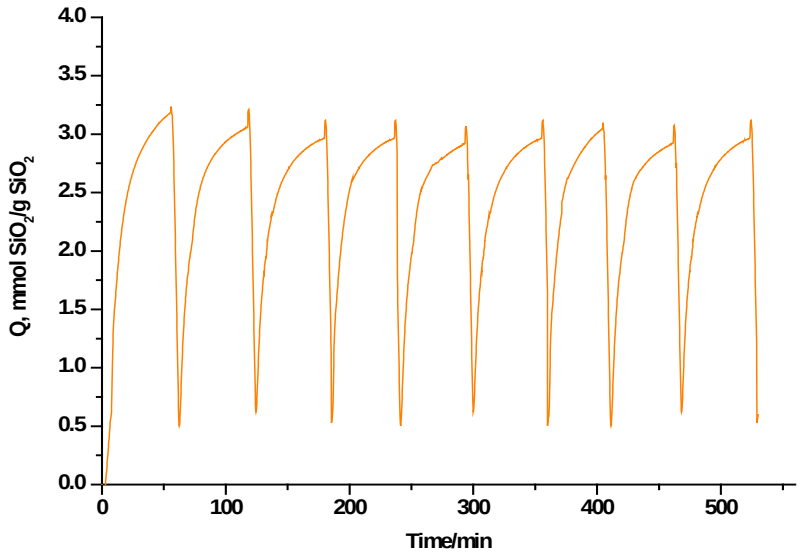

Fig. 8. Adsorption-desorption cycles of CO_2 at 60°C on MCM-41-sil mesoporous material

The small band present on the FTIR spectra around 1484 cm^{-1} in the case of functionalized silica, confirmed the successful grafting of 3-aminopropyl-triethoxy silane used as a functionalization agent. The band present at 1522 cm^{-1} on the FTIR spectra in case of the SSBA-15+N2 graphed sample can be associate with N–H stretching and bending vibrations, respectively, meaning that the grafting process of ethylene diamine (N2) on modified SSBA-15 sample took place. Rope-like structure of these functionalized materials was observed based on the SEM micrograph.

The resulting gases during thermal analysis of the synthesized molecular sieves were identified using mass spectrometry together with thermogravimetry, while CO_2 adsorption capacity of the adsorbent composite was calculated from the mass loss during the desorption step of TG curves using by TPD program. The obtained results for MCM-41- sil (3.32 mmol CO_2/g SiO_2) and SSBA-15+N2 (0.55 n_{CO2} n_{NH2} mmol CO_2/mmol NH_2) concerning the CO_2/NH_2/mmol/mmol values can be considered as promising materials for the possible applications on the CO_2 adsorption-desorption process.

The adsorption–desorption process on the graphed samples was studied for the temperature range 50-80°C. The optimal temperature determined by TPD was found to be 60°C. CO_2 adsorption-desorption cycles showed that MCM-41-sil exhibits a relatively good stability after 9 cycles at a 60°C adsorption temperature. The optimum regeneration steps depend on the temperature of adsorption-desorption process in correlation with the used functionalized agent and tested method.

Acknowledgements

These investigations were partially financed by Romanian Academy Project No. 4.3. and by the Ministry of Education, Science and Technological Development of Republic of Serbia (Project OI172043).

References

Abolfazl J., Seyed A.A.M., Bahamin B., Amin M., (2012), Enhancement in thermal and hydrothermal stability of novel mesoporous MCM-41, *Journal of Porous Materials*, **19**, 979–988.

Ahmeda S., Ramlib A., Yusup S., (2016), CO_2 adsorption study on primary, secondary and tertiary amine functionalized Si-MCM-41, *International Journal of Greenhouse Gas Control*, **51**, 230–238.

Asefa T., Tao Z., (2012), Mesoporous silica and organosilica materials - Review of their synthesis and organic functionalization, *Canadian Journal of Chemistry*, **90**, 1015–1031.

Barbosa M.N., Antonio S.A., Galvao L.P.F.C., Silva E.F.B., Santos G.D., Luz E.G.Jr., Fernandes V.J.Jr., (2011), Carbon dioxide adsorption over DIPA functionalized MCM-41 and SBA-15 molecular sieves, *Journal of Thermal Analysis and Calorimetry*, **106**, 779–782.

Beck J.S., Vartuli J.C., Roth W.J., Leonowic M.E., Kresge C.T., Schmitt K.D., Chu C.T.W., Olson D.H., Sheppard E.W., (1992), A new family of mesoporous molecular sieves prepared with liquid crystal templates, *Journal of the American Chemical Society*, **114**, 10834–10843.

Bollini P., Didas S.A., Jones C.W., (2011), Amine-oxide hybrid materials for acid gas separations, *Journal of Materials Chemistry*, **21**, 15100–15120.

Borcanescu S., Popa A., Verdes O., Suba M., (2019), *Temperature Effect on CO_2 Adsorption-Desorption Process of Different Functionalized Mesoporous Materials*, Proc. 25th Int. Symp. on Analytical and Environmental Problems, 7-8 October, Szeged, Hungary, 105–109.

Carvalho V.L.S., Silva E., Andrade J.C., Silval J.A., Urbina M., Nascimento P.F., Carvalho F., Ruiz J.A., (2015), Low-cost mesoporous adsorbents amines-impregnated for CO_2 capture, *Microporous Adsorption*, **21**, 597–609.

Chen C., Zhang S., Kyung H.R., Ahn W.-S., (2017), Amine–silica composites for CO_2 capture: A short review, *Journal of Energy Chemistry*, **26**, 868–880.

Ciesla U., Schuth F., (1999), Ordered mesoporouse materials, *Microporous and Mesoporous Materials*, **27**, 131–149.

Doadrio A.L., Sousa E.M.B., Doadrio J.C., Pérez Pariente J., Izquierdo-Barba I., Vallet-Reg M., (2004), Mesoporous SBA-15 HPLC evaluation for controlled gentamicin drug delivery, *Journal of Controlled Release*, **97**, 125–132.

Galarneau A., Cambon N., Renzo F. D., Choil M., Fajula F., (2003), Microporosity and connections between pores in SBA-15 mesostructured silicas as a function of the temperature of synthesis, *New Journal of Chemistry*, **27**,73–79.

Gargiulo N., Peluso A., Aprea P., Pepe F., Caputo D., (2014), CO_2 adsorption on polyethylenimine-functionalized SBA-15 mesoporous silica: Isotherms and modeling, *Journal of Chemical and Engineering Data*, **59**, 896–902.

Harja M., Tataru-Farmus R., Droniuc Hultuana E., Gómez de Castro C., Ciobanu G., Lazăr L., (2021), Influence of ethylenediamine content over performance of CO_2 absorption into potassium carbonate solutions, *Environmental Engineering and Management Journal*, **20**, 507–516.

Heydari-Gorji A., Belmabkhout Y., Sayari A., (2011), Polyethylenimine-impregnated mesoporous silica: effect of amine loading and surface alkyl chains on CO_2 adsorption, *Langmuir*, **27**, 12411–12416.

Hiyoshi N., Yogo K., Yashima T., (2005), Adsorption characteristics of carbon dioxide on organically functionalized SBA-15, *Microporous Mesoporous Materials*, **84**, 357–365.

Kamarudin N.H.N., Jalil A.A., Triwahyono S., Salleh N.F.M., Karim A.H., Mukti R.R., Hameed B.H., Ahmad A., (2013), Role of 3-aminopropyltriethoxysilane in the preparation of mesoporous silica nanoparticles for ibuprofen delivery: effect on physicochemical properties, *Microporous Mesoporous Materials*, **180**, 235–241.

Khader M.M., Al-Marri M.J., Ali S., Qi G., Giannelis E.P., (2015), Adsorption of CO_2 on polyethyleneimine 10k-mesoporous silica sorbent: XPS and TGA studies, *American Journal of - Analytical Chemistry*, **6**, 274–284.

Kim D.H., Celedonio J., Ko Y.S., (2017), A study on grafting efficiency of amine and CO_2 sorption behavior inside amorphous silica, *Topics in Catalysis*, **60**, 706–713.

Ma X., Wang X., Song C.J., (2009), "Molecular Basket" sorbents for separation of CO_2 and H_2S from various gas streams, *Journal of the American Chemical Society*, **131**, 5777–5783.

Majda D., Napruszewska B.D., Zimowska M., Makowski W., (2016), Porosity of SBA-15 after functionalization of the surface with aminosilanes, *Microporous Mesoporous Materials*, **234**, 98–106.

Manianglung C., Pacia R.M., Ko Y.S., (2019), Synergistic effect of blended primary and secondary amines functionalized onto the silica on CO_2 capture performance, *Korean Journal of Chemical Engineering*, **36**, 1267–1273.

Maria Chong A.S., Zhou X.S., (2003), Functionalization of SBA-15 with APTES and characterization of functionalized materials, *The Journal of Physical Chemistry B*, **107**, 12650–12657.

Meléndez-Ortiz H.I., Perera-Mercado Y., Mercado-Silva J.A., Olivares-Maldonado Y., Castruita G., García-Cerda L.A., (2014), Functionalization with amine-containing organosilane of mesoporous silica MCM-41 and MCM-48 obtained at room temperature, *Ceramics International*, **40**, 9701–9707.

Mello M.R., Phanon D., Silveira G.Q., Llewellyn P.L., Ronconi C.M., (2011), Amine-modified MCM-41 mesoporous silica for carbon dioxide capture, *Microporous Mesoporous Materials*, **143**, 174–179.

Mukherjee S., Mihra A., Samanta A.N., (2019), Amine-impregnated MCM-41 in post-combustion CO_2 capture: Synthesis, characterization, isotherm modelling, *Advanced Powder Technology*, **30**, 3231–3240.

Popa A., Sasca V., Verdes O., Suba M., Barvinschi P., (2018), Effect of the amine type on thermal stability of modified mesoporous silica used for CO_2 adsorption, *Journal of Thermal Analysis and Calorimetry*, **134**, 269–279.

Rao N., Wang M., Shang Z., Hou Y., Fan G. Li, (2018), CO_2 adsorption by amine-functionalized MCM-41: a comparison between impregnation and grafting modification methods, *CO_2 Energy Fuels*, **32**, 670–677.

Ratchadapiban K., Praserthdam P., Tungasmita D.N., Tangku C., Anutrasakda W., (2018), Effect of surface modifications of SBA-15 with aminosilanes and 12-tungstophosphoric acid on catalytic properties in environmentally friendly esterification of glycerol with oleic acid to produce monoolein, *Catalysts*, **360**, 1–18.

Ridha B.S., Joel M.K., Khaled E., Bahoueddine T., Abdelhamid S., (2020) A unified approach to CO_2–amine reaction mechanisms, *ACS Omega*, **40**, 26125–26133.

Rodrıguez-Estupinan P., Giraldo L., Moreno-Pirajan J.C., (2015), Calorimetric study of amino-functionalised SBA-15, *Journal of Thermal Analysis and Calorimetry*, **121**, 127–134.

Sánchez-Zambrano K.S., Lima Duarte L., Soares M. D.A., Vilarrasa-García E., Bastos-Neto M., Rodríguez-Castellón E., Silva de Azevedo D.C., (2018), CO_2 Capture with mesoporous silicas modified with amines by double functionalization: assessment of adsorption/desorption cycles, *Materials*, **11**, 887–906.

Sanz R., Calleja G., Arencibia A., Sanz-Pérez E.S., (2015), CO_2 capture with pore-expanded MCM-41 silica modified with amino groups by double functionalization, *Microporous Mesoporous Materials*, **209**, 165–171.

Sayari A., Kruk M., Jaroniec M., Moudrakovski I.L., (1998), New approaches to pore size engineering of mesoporous silicates, *Advanced Materials*, **10**, 1376–1379.

Selvam P., Bhatia S.K., Sonwane C.G., (2001), Recent advances in processing and characterization of periodic mesoporous MCM-41 silicate molecular sieves, *Industrial and Engineering Chemistry Research*, **40**, 3237–3261.

Sharma P., Baek I., Park Y., Nam S., Park J., Park S., Park S.Y., (2012), Adsorptive separation of carbon dioxide by polyethyleneimine modified adsorbents, *Korean Journal of Chemical Engineering*, **29**, 249–262.

Sheng X., Kong J., Zhou Y., Zhang Y., Zhang Z., Zhou S., (2014), Direct synthesis, characterization and catalytic application of SBA-15 mesoporous silica with heteropolyacid incorporated into their framework, *Microporous and Mesoporous Materials*, **187**, 7–13.

Son W.J., Choi J.S., Ahn W.S., (2008), Adsorptive removal of carbon dioxide using polyethyleneimine-loaded mesoporous silica materials, *Microporous and Mesoporous Materials*, **113**, 31–40.

Vilarrasa-García E., Cecilia J.A., Santos S.M.L., Cavalcante Jr.C.L., Jiménez-Jiménez J., Azevedo D.C.S., Rodríguez-Castellón E., (2014), CO_2 adsorption on APTES functionalized mesocellular foams obtained from mesoporous silicas, *Microporous Mesoporous*

Materials, **187**, 125–134.

Wang Y., Zibrowius B., Yang C.M., Spliethoff B., Schuth F., (2004), Synthesis and characterization of large pore vinyl-functionalized mesoporous silica SBA-15, *Chemical Communications*, 46–47, https://doi.org/10.1039/B309578A.

Wang X., Chen J.C.C., Tseng Y.-H., Cheng S., (2006), Synthesis, characterization and catalytic activity of ordered SBA-15 materials containing high loadings of diamines functional groups, *Microporous and Mesoporous Materials*, **95**, 57–65.

Yan X., Zhang L., Zhang Y., Yang G., Yan Z., (2011), Amine-modified SBA-15: Effect of pore structure on the performance for CO_2 capture, *Industrial and Engineering Chemistry Research*, **50**, 3220–3226.

Yuan M.-H., Wang L., Yang R.T., (2014), Glow discharge plasma-assisted template removal of SBA-15 at ambient temperature for high surface area, high silanol density, and enhanced CO_2 adsorption capacity, *Langmuir*, **30**, 8124–8130.

Zelenak V., Badanicova M., Halamova D., Cejka J., Zukal A., Murafa N., Goerigk G., (2008), Amine-modified ordered mesoporous silica: Effect of pore size on carbon dioxide capture, *Chemical Engineering Journal*, **144**, 336–342.

Zhang S., Chen C., Ahn W.-S., (2019), Recent progress on CO_2 capture using amine-functionalized silica, *Current Opinion in Green and Sustainable Chemistry*, **16**, 26–32.

Zhao D., Feng J., Huo Q., Melosh N., Fredrickson G.H., Chmelka B.F., Stucky G.D., (1998), Triblock copolymer syntheses of mesoporous silica with periodic 50 to 300 angstrom pores, *Science*, **279**, 548–552.

Zhao D., Huo Q., Feng J., Chmelka B.F., Stucky G.D., (1998), Nonionictriblock and star diblock copolymer and oligomeric surfactant syntheses of highly ordered, hydrothermally stable, mesoporous silica structures, *Journal of the American Chemical Society*, **120**, 6024–6036.